Article

The Investigation of Two-Phase Expansion Performance with Indicator Diagram in a Twin-Screw Expander

Yang Ma [1,*], Yaodong Zhou [2] and Zhenkun Zhu [3]

1 Department of Thermal Engineering, Shandong Jianzhu University, Jinan 250101, China
2 Shanghai Marine Diesel Engine Research Institute, Shanghai 201108, China; zydjshm@163.com
3 Shandong Xianghuan Environmental Technology Co., Ltd., Jinan 250001, China
* Correspondence: myandmyy@163.com

Abstract: Volumetric expanders are proven to be more suitable for small-scale waste heat recovery applications because of their simplicity, reliability, lower rotational speed and lower cost. Unlike turbines, volumetric expanders can work in the two-phase fluid state, which broadens their application fields. To investigate the two-phase performance of volumetric expanders, a specific twin-screw expander was chosen and modeled. The leakage loss and the suction pressure loss were primary concerns in this research. The two-phase expansion process in the expander is presented in detail using the developed mathematical model with an indicator diagram. The influence of several factors, including inlet vapor quality, rotational speed and intake pressure, are investigated. The influence mechanism of the vapor phase and the liquid phase on expander performance is clarified. In brief, this paper presents an illustrative understanding of the two-phase expansion process in twin-screw expanders.

Keywords: waste heat recovery; twin-screw expander; two-phase expansion; low grade heat

1. Introduction

Along with the increasing demand for clean energy and more strict CO_2 emission constraints, low-grade heat sources, such as industrial waste heat, geothermal heat [1] and solar heat [2], have attracted more and more attention from engineers and researchers. Improving the conversion efficiency of low-grade waste heat resources is a key issue for energy saving. Currently, the lack of efficient and suitable expanders has become a technical bottleneck for low-grade heat conversion [3].

Generally, expanders [4] can be classified into two categories: dynamic expanders (turbines) and volumetric expanders [5], such as scroll expanders [6,7] and screw expanders [8,9]. The turbines are usually suitable for superheated working fluids and large capacity applications, while the volumetric expanders are more appropriate for small-scale waste heat recovery applications. So far, numerous ORC (organic Rankine cycle) researchers have shown interest in the volumetric expanders. Muhammad et al. [5] reviewed volumetric expanders for waste heat recovery applications. The comparative assessment, based on performance, current market status and economics, showed that screw expanders and scroll expanders are most suitable choices. Lemort et al. [10] tested and modeled a scroll expander integrated into an organic Rankine cycle with working fluid R123. In a follow-up paper [11], they presented a global ORC model based on the scroll expander model. This model was used to investigate potential improvements to the prototype. Inspired by Lemort et al., Giuffrida [12] improved the semi-empirical model of a single-screw expander for the organic Rankine cycle. Zhu et al. [13] also experimentally tested the performance of a scroll expander with R123. They also developed a numerical model to predict the state parameters in expansion chambers and the performance of the scroll expander. Smith et al. [14] conducted a series of research studies on screw expanders

for power recovery, including the modeling, performance calculation and application of screw expanders. Tang et al. [15] studied the performance of a twin-screw expander theoretically and experimentally in a geothermal organic Rankine cycle power plant. The effect of several important factors, including rotating speed, intake pressure and inlet superheat, on the expander's performance were investigated. Iva et al. [16] performed a 3D CFD analysis of a twin-screw expander. The simulation results showed that the largest pressure drop was caused by throttling loss at the intake port and, therefore, the design of the intake port needs to be optimized. In another paper, Iva et al. [17] concluded that the pressure pulsation in the intake port affected both the aeroacoustics in that domain and the noise generated mechanically by rotor rattling. He et al. [18] experimentally tested the performance of a single screw expander. Their results showed that satisfactory power output and economic performance could be obtained at high suction pressure and high rotating speed, while still maintaining good efficiency. Lei et al. [19] proposed a new idea for single screw expanders. They converted the single screw expander into a double-stage machine in large expansion conditions by utilizing the discharge velocity of screw grooves. The new structure of the expander seemed to eliminate under-expansion loss.

It should be noticed that one important advantage of volumetric expanders is that this type of expander is also workable under total-flow expansion or two-phase expansion conditions, which make it more promising in the low-grade heat recovery field. Therefore, volumetric expanders, especially screw expanders, can be used for low vapor quality geothermal fluid heat recovery or some new types of ORCs, such as the trilateral cycle [20] and partial evaporating ORC [21–23], which need two-phase expanders. Taniguchi et al. [24] presented a numerical model to predict the performance of a two-phase flow screw expander. Wu et al. [25] studied the trilateral flash cycle (TFC) by means of numerical modeling. In their research, the flash evaporating rate was introduced into a model of the two-phase expansion process in the reciprocating expander with a cyclone separator. Smith [26] investigated total-flow systems involving two-phase expansion. It was concluded that, in some cases, a single screw expander could be utilized for the two-phase expansion process to produce greater power outputs than would be possible from dry vapor expansions in turbines. Smith [27,28] also carried out an extensive research and development program to improve the understanding of how twin-screw expanders may be used to recover power from two-phase expansion processes. It was confirmed that the initial filling of the volume formed by the rotors and the casing caused a relatively large pressure drop. Xia et al. [29] investigated the performance of a single-screw expander with different intake dryness fractions. The experimental results showed that, with the increase of intake dryness fractions, the power output and expansion ratio were increased; however, the overall efficiency decreased. Alexander Nikolov et al. [30] provided a basic approach addressing the two-phase mass flow rate calculation in water-flooded twin-screw machines. Based on a generic inlet-geometry model, two-phase mass flow rates were recorded for different operating conditions and mass dryness fractions. Bianchi et al. [31,32] presented a numerical chamber model of a two-phase twin-screw expander and its further integration into a one-dimensional model of a TFC system for low-grade heat to power conversion applications. Parametric analysis on several degrees of freedom of the full TFC system concluded that expander speed and BIVR are the variables that mostly impact the net power output of the unit.

However, few researchers have shown concern about the effect of inlet vapor quality. The inlet vapor quality is supposed to have a vital effect on the performance of an expander. The mass flow rate, power output, isentropic efficiency, and pressure changes are all affected by the inlet vapor quality. Although the calculation of two-phase flow in the expander may not be so accurate, some preliminary analysis can be done at this time. Therefore, a specific screw expander is investigated for its two-phase expansion performance in this paper. The investigation mainly focuses on the suction pressure loss and leakage loss, as they are the primary causes for loss in screw expanders. The two-phase expansion process in the expander is presented in detail using a mathematical model developed with

indicator diagrams. The mathematical model was mainly inspired by Taniguchi [24], with some modifications to the two-phase mass flow rate calculation. This paper facilitates a better understanding of the two-phase expansion in the screw expander and a reference for performance prediction.

2. Materials and Methods

2.1. Screw Expander Geometric Model

The construction of a screw expander is illustrated in Figure 1. The screw expander is mainly composed of a pair of screw rotors, cylinders, bearings, synchronous gears, seal assemblies and couplings. The helical female and male rotors that are in mesh with each other rotating in opposite directions are placed in parallel in the cylinder. One working cycle of the screw expander consists of three processes, namely, the intake phase, the expansion phase and the exhaust phase. In the intake phase, a pair of lobes of the female and male rotors are separated at the intake end, and the working fluid flows into the inter-lobe space through the intake port. The force exerted on the rotor by the working medium pushes the male and female rotors to rotate continuously. The intake phase ends when the inter-lobe space is separated from the intake port. Then, the expansion phase starts. The increasing working volume causes the working fluid to expand continually. When the forward lobes reach the exhaust port, the exhaust process starts. The working fluid flows out until all the working fluid is discharged. In this way, one working cycle is completed.
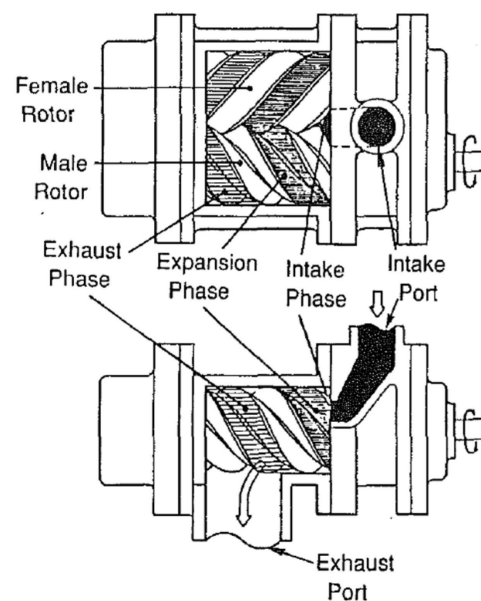
**Figure 1.** The construction of a twin-screw expander [24].

2.1.1. Geometric Parameters

The screw expander discussed in this paper is a SEPG500 type twin screw expander. The rotor profile is SRM-D. The basic geometric parameters are shown in Table 1.

The variations of the working chamber's volume and intake port area, in terms of the rotation angle, are shown in Figure 2. To be specific, the intake end angle was 134° and the discharge start angle was 384°.

Table 1. Basic geometric parameters of SEPG500 twin screw expander.

Designation	Unit	Male Rotor	Female Rotor
Rotor profile		modified asymmetric SRM	
Lobes		4	6
Wrap angle	°	300	200
Outer diameter	mm	510	510
Length of the rotor	mm	840	840
Volume ratio		4.05	
Contact line clearance	mm	1	1
Gear tip clearance	mm	0.7	0.7
Suction and exhaust end face clearance	mm	0.5	0.5
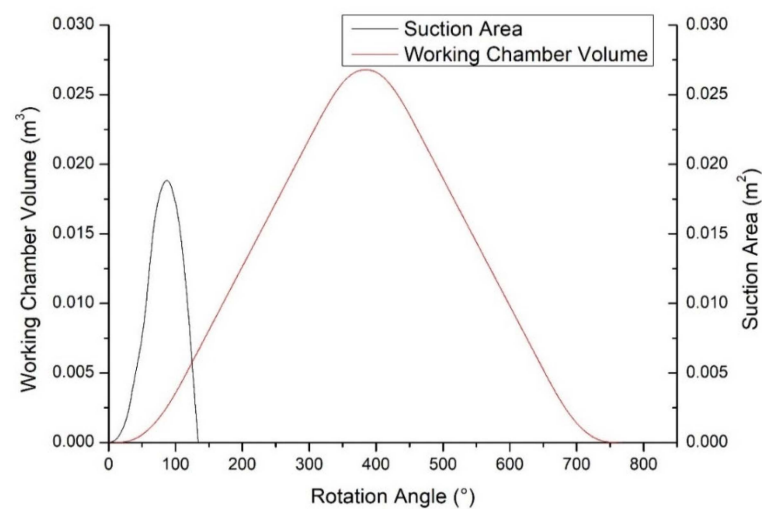
Figure 2. The volume of the working chamber and the intake port area.
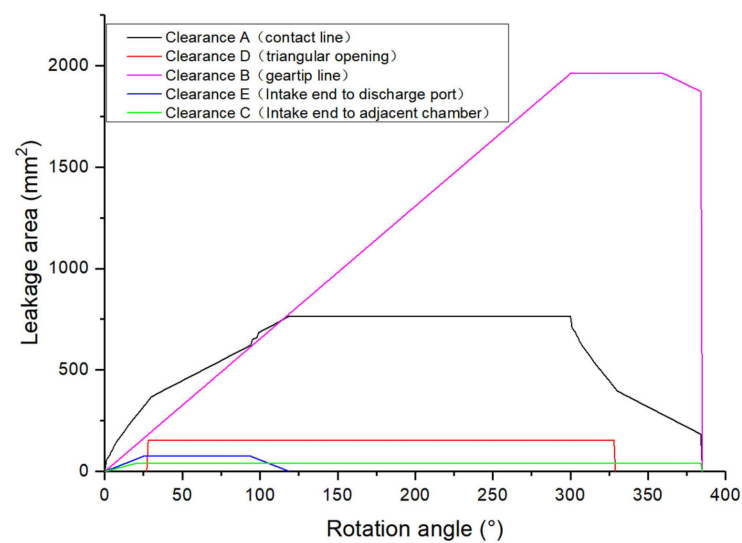
2.1.2. Leakage Paths

There must be certain gaps between all moving parts. In the screw expander, they are mainly between the female and male rotors and between the rotors and the casings. The inherent leakage paths in the screw expander are shown in Figure 3.
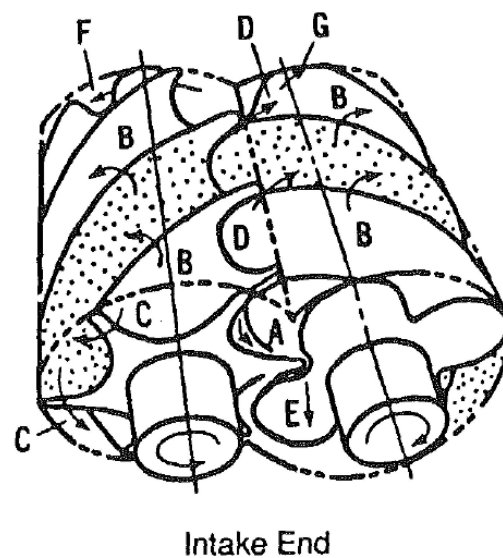
Figure 3. Screw expander leakage paths [24].

Leakage path A refers to the clearance between male and female rotors, the so-called contact line. The working fluids flow directly to the discharge chamber through this leakage path. In this case, the working fluids are discharged without doing any work. Leakage path B refers to the gear tip line between rotor and casing. The working fluids flow to the adjacent chambers through this leakage path. That means the working fluids in the object working chamber flow to the lower-pressure chamber, while the working fluids in the higher-pressure chamber also flow to the object working chamber. The thermal properties of working fluids in these two adjacent working chambers are the states of $\pm 90°$ in terms of rotation angle. Leakage path D refers to the triangular opening formed by the rotors and the casing. The working fluids also flow to the adjacent chambers through this leakage path. Leakage paths C and E refer to the clearance between the rotor charge ends and the casings. Specifically, C refers to the leakage between adjacent chambers and E refers to the leakage between the working chamber and the discharge port. Leakage paths F and G refer to the clearances between the rotor discharge ends and the casings. In this paper, the leakage at the discharge end is ignored, since the pressure is relatively low and the leakage time is also very short.

The areas of these leakage paths above were measured in pro/E5.0 (CAD design software developed by PTC company) and are presented in Figure 4. The leakage area through which the working fluid flows into the object working chamber was 90° behind the outward flow. All the leakage flows disappeared when the working chamber started to discharge.

Figure 4. Leakage areas of the leakage paths.

2.2. Two-Phase Expansion Model

2.2.1. Thermodynamic Process Modeling

To simplify the calculation, some assumptions were made, as follow:

1. The two-phase working fluid was always at thermodynamic equilibrium state.
2. The gravitational potential energy and kinetic energy change were ignored.
3. The whole process was assumed to be adiabatic.

In this model, the leakage loss, heat transfer loss and suction pressure loss were considered for the entire working cycle. The mechanical and frictional loss is considered separately in Section 2.2.3.

All the variables were the function of time in this model.

Intake Phase

The mass balance in the working chamber during intake phase can be expressed as:

$$\rho(t)V(t) = \rho(t - \Delta t)V(t - \Delta t) + \Delta G_{int} + \Delta G_{lk,in} - \Delta G_{lk,out} \tag{1}$$

V is the working volume, which can be derived from Figure 2. ΔG_{int} and ΔG_{lk} are the intake mass and leakage mass for small time step, Δt. The time step Δt here is taken as the time for the male rotor to turn an angle of $1°$. Therefore, all the variables are also the function of rotation angle.

The energy balance in the working chamber can be expressed as:

$$\rho(t)V(t)u(t) + p(t - \Delta t)[V(t) - V(t - \Delta t)] = \\ \rho(t - \Delta t)V(t - \Delta t)u(t - \Delta t) + \Delta G_{int}h_{int} + \Delta G_{lk,in}h_{lk,in} - \Delta G_{lk,out}h_{lk,out} \tag{2}$$

For two-phase fluids, the density, specific internal energy, specific enthalpy and specific entropy are calculated by:

$$\rho_{tp} = x\rho_g + (1 - x)\rho_l \tag{3}$$

$$\rho_{tp}u_{tp} = x\rho_g u_g + (1 - x)\rho_l u_l \tag{4}$$

$$\rho_{tp}h_{tp} = x\rho_g h_g + (1 - x)\rho_l h_l \tag{5}$$

The thermal parameters of the saturated state are only a function of pressure. Therefore, the specific enthalpy, vapor quality and pressure can be obtained according to the density and specific internal energy, given by:

$$[h(t), x(t), p(t)] = f[\rho(t), u(t)] \tag{6}$$

Expansion phase

The governing equations during the expansion phase are obtained by simply setting $\Delta G_{int} = 0$. The mass balance in the working volume is given by:

$$\rho(t)V(t) = \rho(t - \Delta t)V(t - \Delta t) + \Delta G_{lk,in} - \Delta G_{lk,out} \tag{7}$$

The energy balance in the working chamber can be expressed as:

$$\rho(t)V(t)u(t) + p(t - \Delta t)\Delta V = \rho(t - \Delta t)V(t - \Delta t)u(t - \Delta t) + \Delta G_{lk,in}h_{lk,in} - \Delta G_{lk,out}h_{lk,out} \tag{8}$$

The remaining computational procedures are the same as for the intake phase.

Exhaust phase

In a real screw expander, the discharge port area is very large to reduce the exhaust pressure loss. Hence, the pressure in the working volume can be taken as equal to the exhaust pressure during the exhaust phase for simplification. Therefore, the exhaust phase was not modeled in detail in this paper.

2.2.2. Two-Phase Flow Mass Flow Rate Calculation

During the working process, working fluid flows in and out through the intake port, the discharge port and the leakage paths. The mass flow rate of the two-phase fluid needs to be modeled. A separate phase model was considered in this paper, which ignored the interaction of the two phases.

The isentropic nozzle relationship for subsonic and choked regimes are applied for mass flow rate calculation of gas, which can be expressed as:

$$
\dot{m}_g = \begin{cases} C\alpha A p_1 \sqrt{\dfrac{2k}{(k-1)R_g T_1}\left[\left(\dfrac{p_1}{p_2}\right)^{\frac{2}{k}} - \left(\dfrac{p_2}{p_1}\right)^{\frac{k+1}{k}}\right]} & \left(\dfrac{2}{k+1}\right)^{\frac{k}{k-1}} \leq \dfrac{p_2}{p_1} \leq 1 \\[3ex] C\alpha A_g p_1 \sqrt{\dfrac{2k}{(k+1)R_g T_1}\left(\dfrac{2}{k+1}\right)^{\frac{2}{k-1}}} & 0 \leq \dfrac{p_2}{p_1} \leq \left(\dfrac{2}{k+1}\right)^{\frac{k}{k-1}} \end{cases}
\tag{9}
$$

Symbol C represents the flow coefficient, which needs to be determined, and A is the flow area, which can be obtained from the expander geometrics, as shown in Figures 2 and 4. The subscripts 1 and 2 represent a high-pressure region and a low-pressure region, respectively. The symbol α is the void fraction, which can be calculated by:

$$
\alpha = \left(1 + \frac{1-x}{x}\frac{\rho_g}{\rho_l}S\right)^{-1}
\tag{10}
$$

The symbol S is the slip ratio, which is defined as the flow velocity ratio of the gas phase and the liquid phase and can be calculated according to Smith's model [33]:

$$
S = 0.4 + 0.6\left(\frac{\rho_l}{\rho_g} + 0.4\frac{1-x}{x}\right)^{0.5}\left(1 + 0.4\frac{1-x}{x}\right)^{0.5}
\tag{11}
$$

The mass flow rate of the liquid phase is calculated according to the relationship between the gas and liquid phases, which is:

$$
\frac{\dot{m}_g}{\dot{m}_l} = \frac{x}{1-x}
\tag{12}
$$

For the intake mass flow rate, the subscripts 1 and 2 in the Equation (9) represent for the intake flow and the object working volume, respectively. For leakage mass flow rates, the subscripts 1 and 2 in the Equation (9) represent the object working volume and the reference working volume. The information about the leakage model is listed in Table 2.

Table 2. Leakage model information.

Clearance	Leakage Situation	Reference Working Volume	Leakage Phase
A, E	Outwards	Exhaust port	Two-phase
B, C, D	Inwards and outwards	$\pm 90°$ of male rotor angle	Two-phase
F, G		Not considered	

2.2.3. Other Losses

Mechanical and frictional losses mainly occur in the bearings, shaft seals, rotor gear tips and casing. They are the function of the rotational speed and many other factors, such as bearing load. For simplification, the total losses are assumed to be proportional to the rotational speed [10]. They account for 7 percent of the isentropic power at 3000 r/min [24]. This assumption was considered to be fair because the magnitudes of mechanical and frictional losses were not the consideration in this paper. Therefore, the mechanical losses are estimated by:

$$
\dot{W}_m = 7\% P_s \cdot \frac{N}{3000}
\tag{13}
$$

P_s is the isentropic power of the expander.

2.2.4. The Performance Calculation of the Screw Expander

The performance of the screw expander can be assessed by the isentropic efficiency, delivery rate and power output. These performance indicators can be calculated by the following equations.

First, the actual intake mass flowrate can be calculated by the following equation:

$$Q_{int} = \frac{G_{int} z_{mr} N}{60} \tag{14}$$

where, G_{int} is the actual intake mass flow per working cycle, z_{mr} is the number of lobes of the male rotor and N is the rotate speed of the male rotor.

G_{int} is the summation of intake mass flows:

$$G_{int} = \sum_{is}^{ie} \Delta G_{int} \tag{15}$$

The theoretical intake mass flow rate can be expressed as:

$$Q_{th} = \frac{V_{ie} \rho_{int} z_{mr} N}{60} \tag{16}$$

V_{ie} is the volume of the working chamber when the intake phase ends and ρ_{int} is the intake density of the working fluid.

Then, the filling factor, or delivery rate, is defined as the ratio of the actual intake mass flowrate and the theoretical intake mass flow rate:

$$\lambda = \frac{Q_{int}}{Q_{th}} \tag{17}$$

The indicated expansion work of the working chamber equals the area in the P-V diagram and can be calculated by:

$$w_{ind} = \oint p dV \tag{18}$$

The isentropic expansion work of the working chamber can be expressed as:

$$w_s = G_{int} \left(h_{int} - h'_{ex} \right) \tag{19}$$

h_{int} is the intake enthalpy of the working fluid and h'_{ex} is the enthalpy at the exhaust pressure through the isentropic process.

Then, the indicated isentropic efficiency of the expander is defined as the ratio of the indicated work and the isentropic work:

$$\eta_{i,s} = \frac{w_{ind}}{w_s} \tag{20}$$

The isentropic and indicated output powers of the expander are calculated by Equations (21) and (22), respectively.

$$P_s = w_s \cdot z_{mr} \cdot N/60 \tag{21}$$

$$P_{ind} = w_{ind} \cdot z_{mr} \cdot N/60 \tag{22}$$

The effective power is calculated by:

$$P_{eff} = P_{ind} - P_m \tag{23}$$

P_m represents mechanical losses, including hydraulic frictional loss, acceleration loss and other mechanical losses.

The effective isentropic efficiency is given by:

$$\eta_{e,s} = \frac{P_{eff}}{P_s} \tag{24}$$

2.2.5. The Solution Procedure

Since accurate values for the pressure difference between adjacent working volumes are not initially known, ΔG_{lk} is set equal to zero during the first iteration. Then the working volume pressure in each iteration is set to the value calculated in the previous round. The calculations repeat until the pressure values calculated in the two adjacent iterations are basically unchanged. This constraint condition can be expressed as $\left| p_{change} \right| / p \leq ER_{max}$, where p_{change} is the difference between the final pressures of the last two iterations and ER_{max} is the maximum allowable relative error.

The solution procedure is presented in Figure 5 and was run in MATLAB. All the thermodynamic properties were calculated by means of REFPROP 9.1 [34].
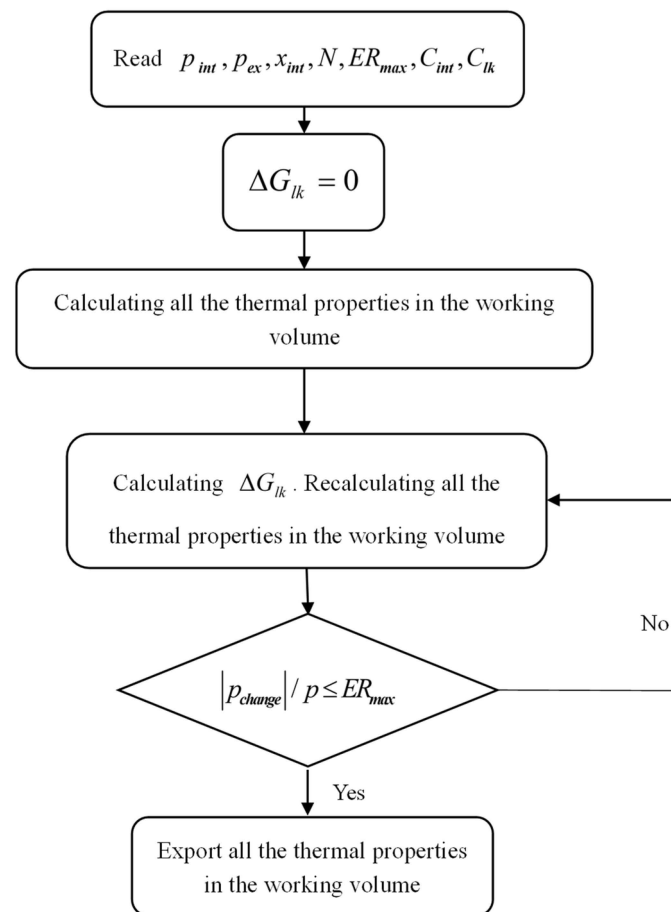
Figure 5. The solution procedure of the thermodynamic model.

3. Results

In this section, the working process of the expander is, first, presented in detail. Then, the influence factors, including inlet vapor quality, rotating speed and intake pressure, are investigated. The working fluid discussed in this paper was R245fa. R245fa is a dry fluid. The main difference between wet fluids and dry fluids is that wet fluids form liquid droplets during the expansion process, while dry fluids do not form droplets.

The flow coefficients for the intake and the leakage process should be determined by means of experimental data. The intake coefficient can be determined by the actual intake mass flow rate and the leakage coefficient can be determined by the measured power indicated. The flow coefficients are related to the construction of the expander, working fluid type and operational conditions. Taniguchi et al. [24] determined that, for R12 in a two-phase screw expander, the intake coefficient was in the range of 0.72–0.76 and the leakage coefficient was in the range of 0.35–0.65. Nikolov et al. [35] determined the intake

coefficient to be in the range of 0.45–0.8 and the leakage coefficient in the range of 0.2–0.8 for R245fa in an oil flooded screw expander. In this paper, the intake coefficient was taken to be 0.76 and the leakage coefficient was 0.5.

The necessary parameter ranges and investigating conditions of R245fa are listed in Table 3.

Table 3. Investigating conditions and flow coefficients of R245fa.

	C_{int}	C_{lk}	p_{int}	p_{ex}	N	x_{int}
value	0.72	0.5	700–1300 kPa	200 kPa	500–2500 rpm	0.1–0.9

3.1. The Working Process of the Expander

The ideal working process of the expander is isobaric suction, isentropic expansion and isobaric exhaust. However, in practice, due to suction pressure loss and leakage loss, the practical process deviates from the ideal process. The P-V diagram of a practical expander is shown in Figure 6.
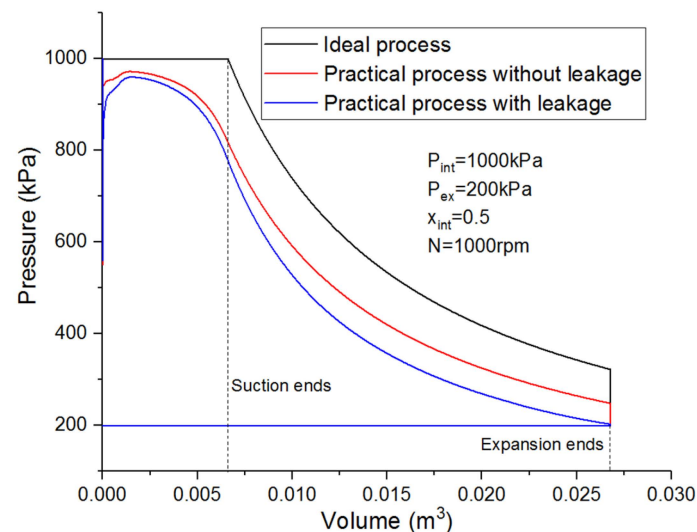
Figure 6. The working process of the working chamber (water).

The working conditions were $x_{int} = 0.5$, $P_{int} = 1$ MPa, $P_{ex} = 0.20$ MPa, N = 1000 rpm. R245fa was the working fluid in the expander.

During the intake phase, the pressure drop cannot be neglected. The addition of the liquid phase makes the pressure drop more serious because of its large density. Along with the rotation of the rotor, the intake port area decreases but the working volume still increases. Thus, at the later stage of the intake phase, pre-expansion occurs, causing a more serious drop in pressure.

The leakage process causes a drop in pressure during both the intake process and the expansion process. The leakage situation in the expander is presented in Figure 7. The leakage through the triangular opening and the rotor charge end was very small in this investigation. Therefore, in order to illustrate leakages more clearly, those leakages are not presented in the figure. A negative value refers to leakage outside, while a positive value refers to leakage into the working volume. It can be seen clearly that, at the early stage, the leakage through the contact line was the most serious of all the leakage paths because of the relatively larger pressure difference between the pressure in the working volume and the discharge pressure. With expansion, the pressure in the working volume decreased, and the leakage area between the casing and the gear tip became larger. Therefore, the leakage through the contact line became smaller, while the leakage through the gear tip line became the primary leakage.
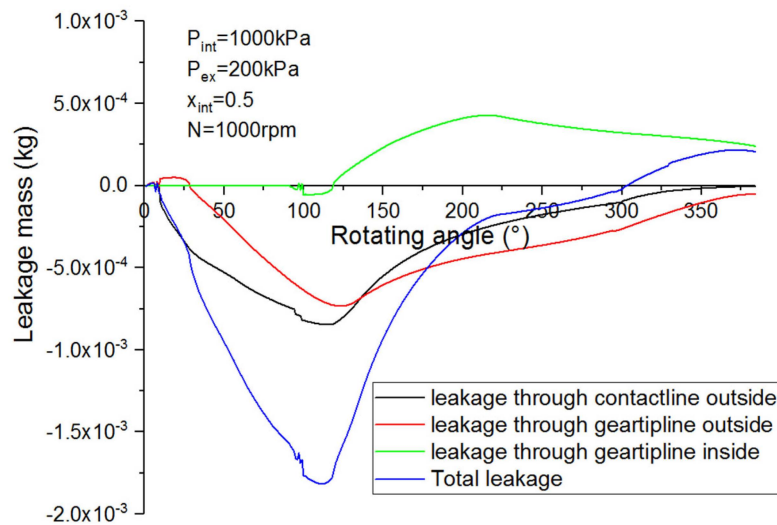
Figure 7. The leakage situation of the working chamber.

In the intake phase and in the early stage of the expansion phase, the pressure in the working volume was quite a lot higher. Hence, the leakage outside was far more serious than the leakage inside. The overall leakage flowed outwards. However, with expansion, the pressure in the working volume decreased and the overall leakage flowed inwards.

The mass variation in the working volume is presented in Figure 8. The total mass in the expansion phase decreased at first and increased at the end, which corresponded to the leakage situation. Although leakage occurred, the vapor mass increased throughout the expansion phase. This was because the flash evaporation vapor amount was much larger than the leakage amount. For the liquid mass, the effect of flash evaporation and leakage need to be considered together. In this case, the liquid mass accounted for much of the total mass. Therefore, the liquid mass variation was similar to the total mass.
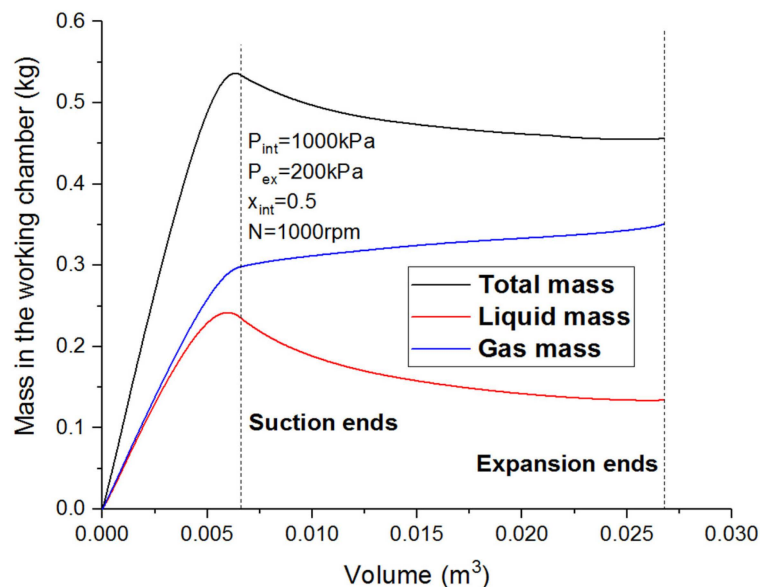
Figure 8. The mass variation in the working chamber (water).

Figure 9 shows the variation of the vapor quality in the expander. Due to the pressure drop, the flash evaporation happened at the beginning of the intake phase, which led to an increase in the vapor quality. It can be seen from the figure that the vapor quality apparently increased before the expansion phase started because of the pre-expansion in the intake phase. In the expansion phase, the vapor quality increased continuously along

with the expansion process. The change rate was larger at the beginning and smaller at the end of the expansion phase.
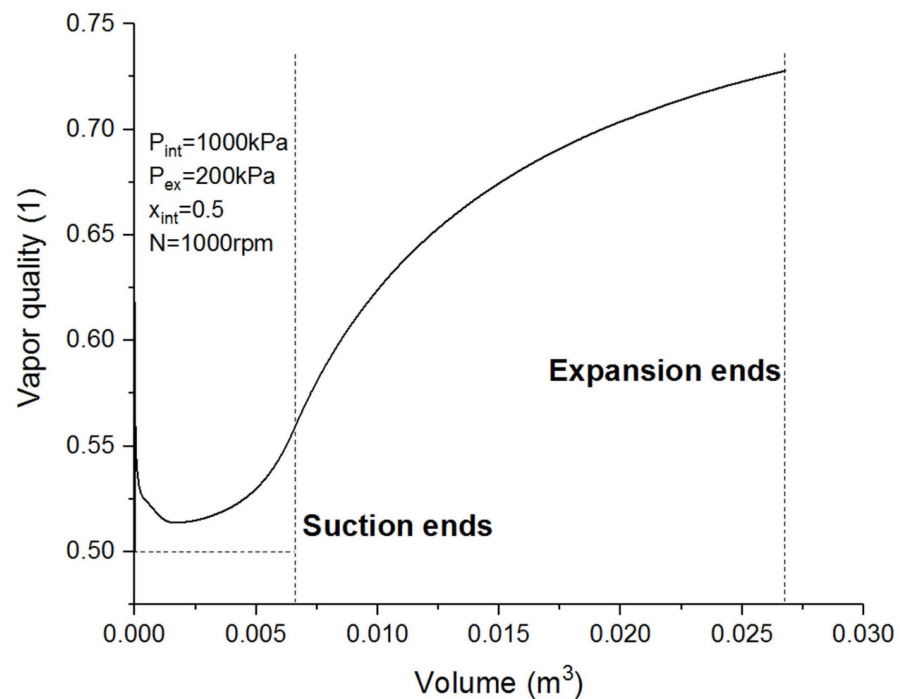
Figure 9. The variation of vapor quality in the working chamber (water).

3.2. The Influence of Inlet Vapor Quality

The influence of inlet vapor quality on the expander is investigated in this section.

Figure 10 shows the influence of inlet vapor quality on the working process of the expander. It can be seen that the pressure loss was larger for lower vapor quality because of the larger density. The pressure at the end of the expansion phase was higher for lower inlet vapor quality, since, for lower vapor quality, the mass of the liquid is larger and, hence, the amount of vapor produced from flash evaporation is also larger, which mitigates the pressure drop during expansion. It can be seen that, when the inlet vapor quality was 0.3 or higher, the influence of inlet vapor quality on the working process was fairly small, as there was little change in the void fraction when the vapor quality was large enough.

Figures 11–13 show, in the working volume, the variation of total mass, vapor mass and liquid mass for R245fa. Figure 14 shows the vapor quality variation in the working volume depending on different inlet vapor qualities. It can be clearly seen that lower vapor quality led to larger intake total mass. However, the intake vapor mass had nearly no relation with the inlet vapor quality. The reason for this was that, for a constant volumetric flow rate, the vapor accounted for most of the total intake volume and the ratio changed little for different vapor qualities.
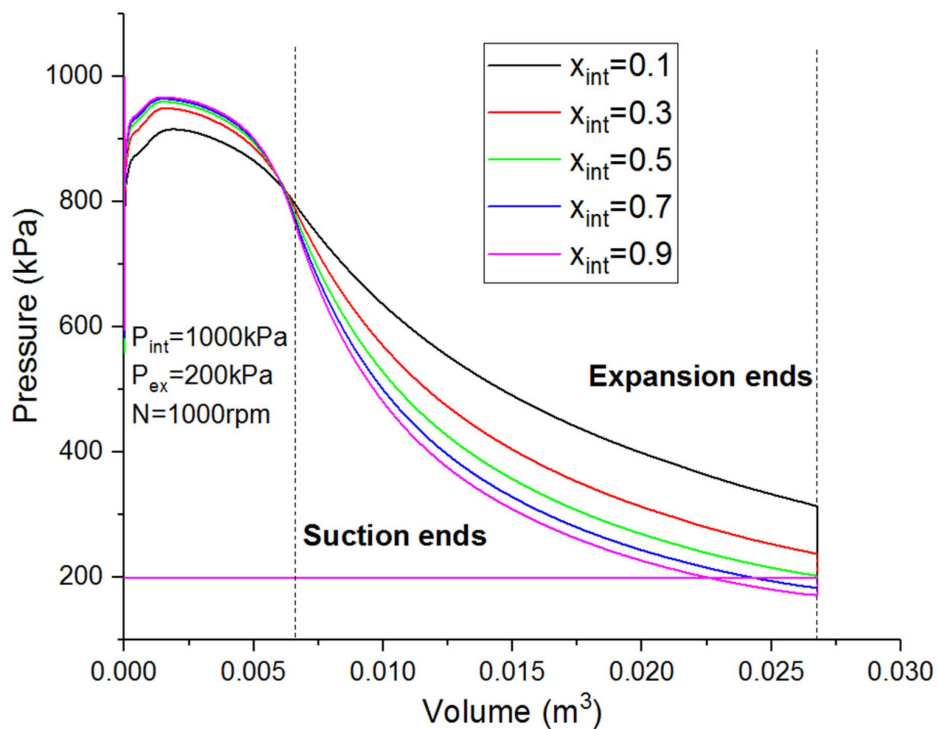
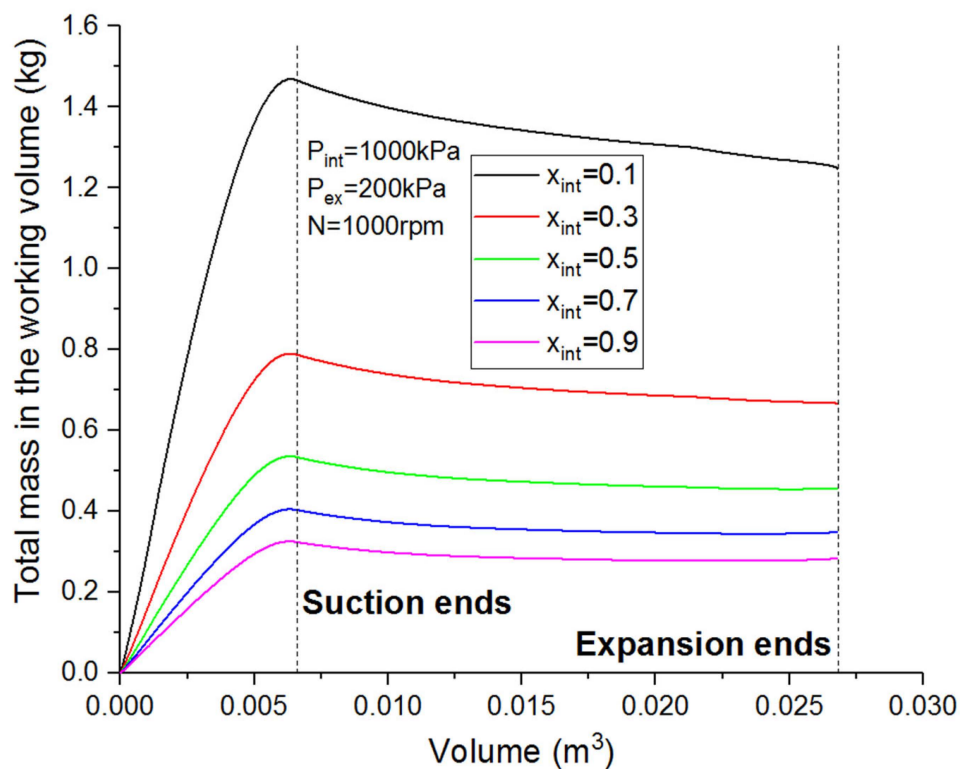**Figure 10.** The influence of inlet vapor quality on working process.

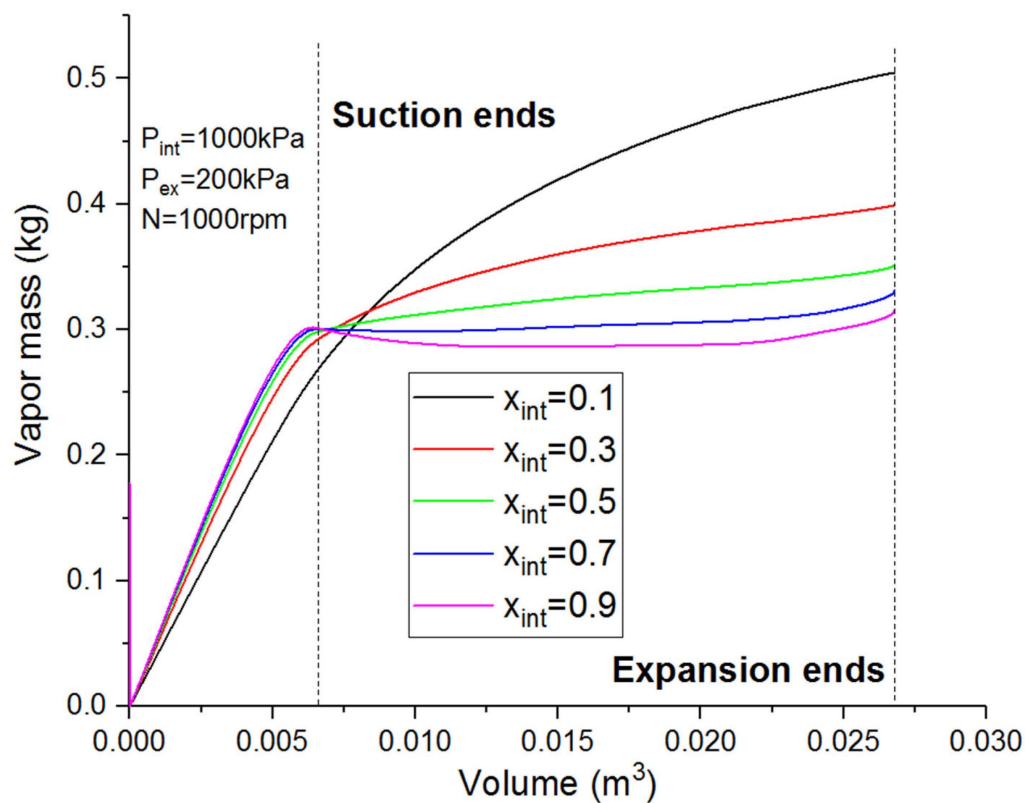**Figure 11.** The influence of inlet vapor quality on total mass.

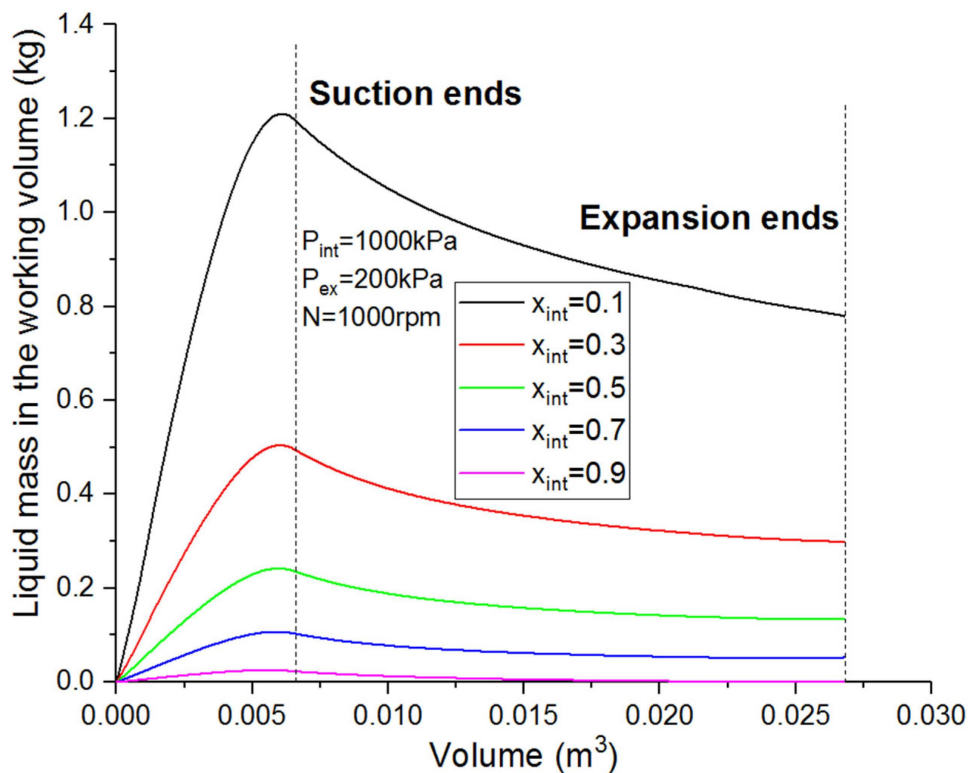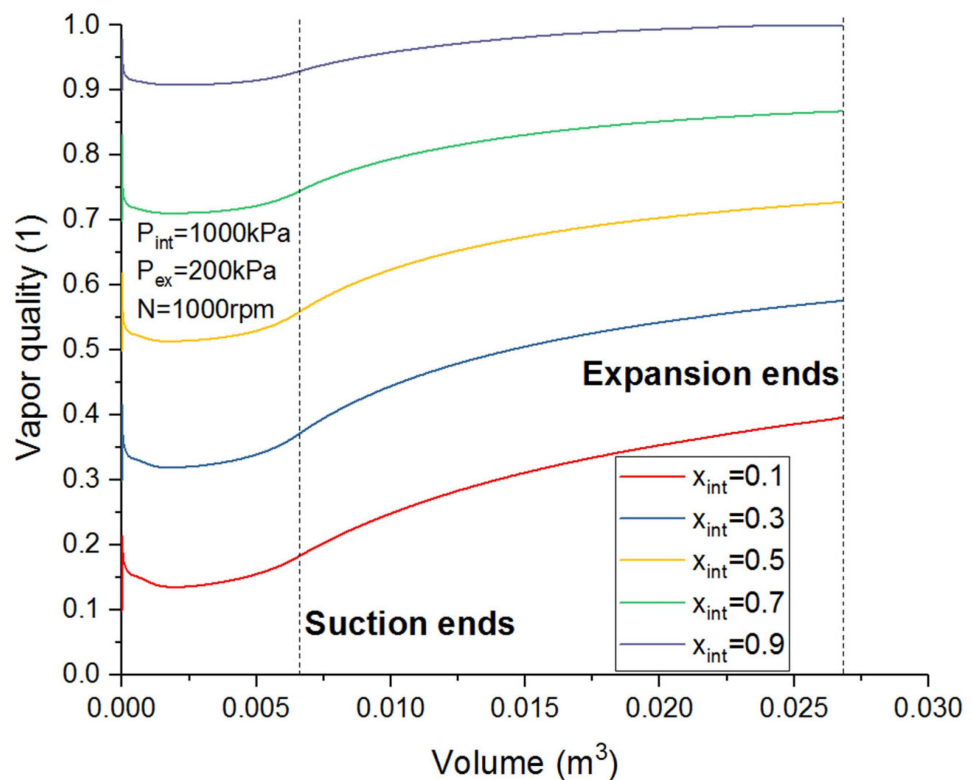**Figure 12.** The influence of inlet vapor quality on vapor mass.

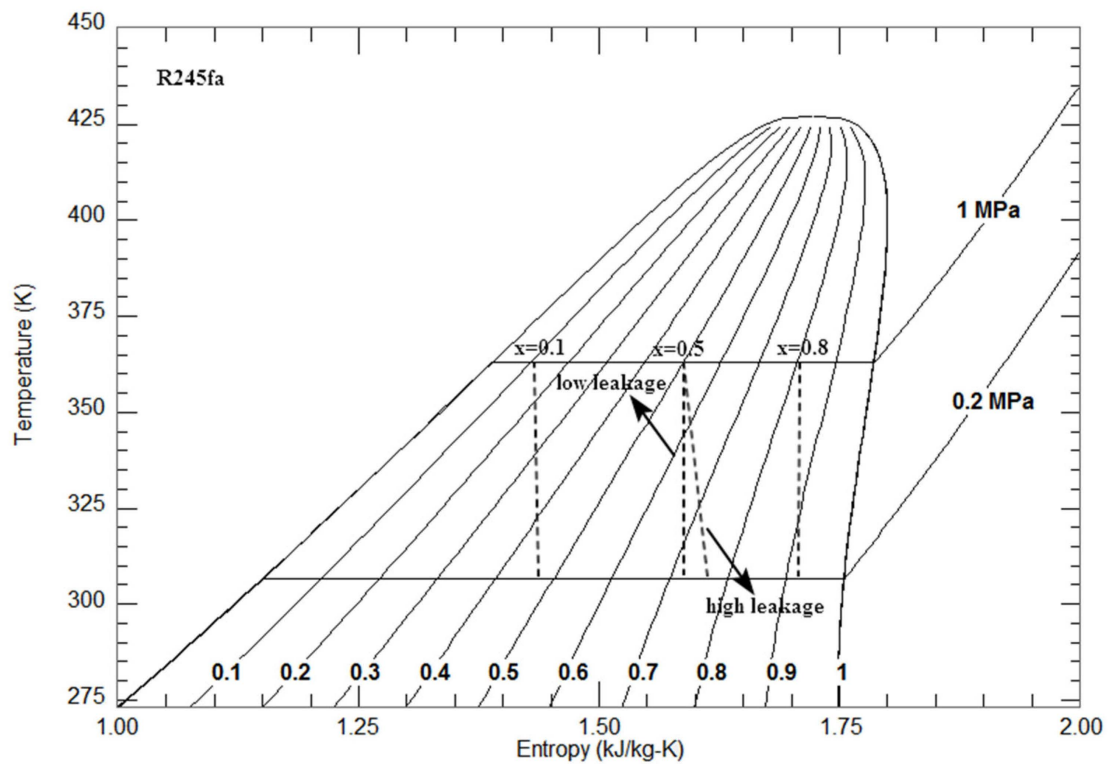**Figure 13.** The influence of inlet vapor quality on liquid mass.

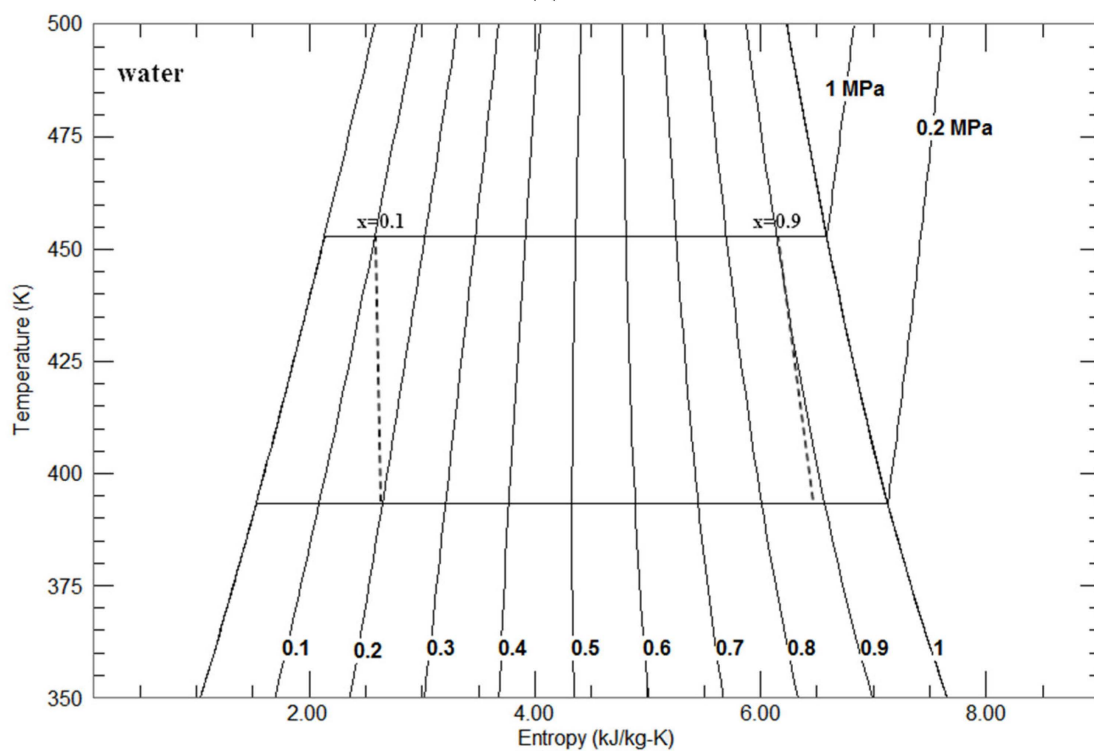**Figure 14.** The influence of inlet vapor quality on the vapor quality variation.

The variations of the vapor mass and liquid mass in the expansion phase are also very interesting. For wet fluids, such as water, the vapor mass increases and the liquid mass decreases during expansion for lower inlet vapor quality, while for higher inlet vapor quality, the contrary is the case. That is because for lower vapor quality, flash evaporation plays the dominating role. For higher vapor quality, more vapor is condensed into liquid than flash vapor. However, for dry fluids, such as R245fa, the vapor is not condensed into liquid. Therefore, the liquid mass always decreases and the vapor mass always increases, regardless of the inlet vapor quality. The vapor quality variation for wet and dry fluids can be more clearly illustrated by the T-s diagram in Figure 15.

It should be noticed that the leakage situation influences the vapor quality variation. Figure 16 shows the influence of different leakage flow coefficients on vapor quality variation in the expander. The more serious the leakage situation, the higher the vapor quality. A more serious leakage situation leads to a more serious process of entropy production, which increases the vapor quality, as shown in Figure 16.

Figure 17 shows the influence of inlet vapor quality on the isentropic efficiency. It should be noted that, for lower inlet vapor quality, under-expansion happens, which means the isentropic efficiency could be higher for full expansion. Therefore, the isentropic efficiencies of fixed exhaust pressure and full-expansion state are both shown in Figure 17 for comparison. The result showed that, under the full-expansion state, the lower vapor quality led to higher isentropic efficiency. This conclusion was consistent with the experimental data in Ref. [29]. Note also that the work was mainly produced by the vapor phase. So, for lower vapor quality, less vapor leaked through the clearance, which led to less irreversible loss. Therefore, the isentropic efficiency was higher for lower inlet vapor quality. A more liquid phase better prevents leakage (smaller leakage flow coefficient), which was not considered in this paper, and which would also contribute to the higher isentropic efficiency. As for delivery rate, higher vapor quality led to a higher delivery rate, as shown in Figure 18. The vapor phase of lower density fills the volume better than the liquid phase.

(**a**)

(**b**)

Figure 15. The illustration of vapor quality variation. (**a**) R245fa (dry fluids); (**b**) Water (wet fluids).
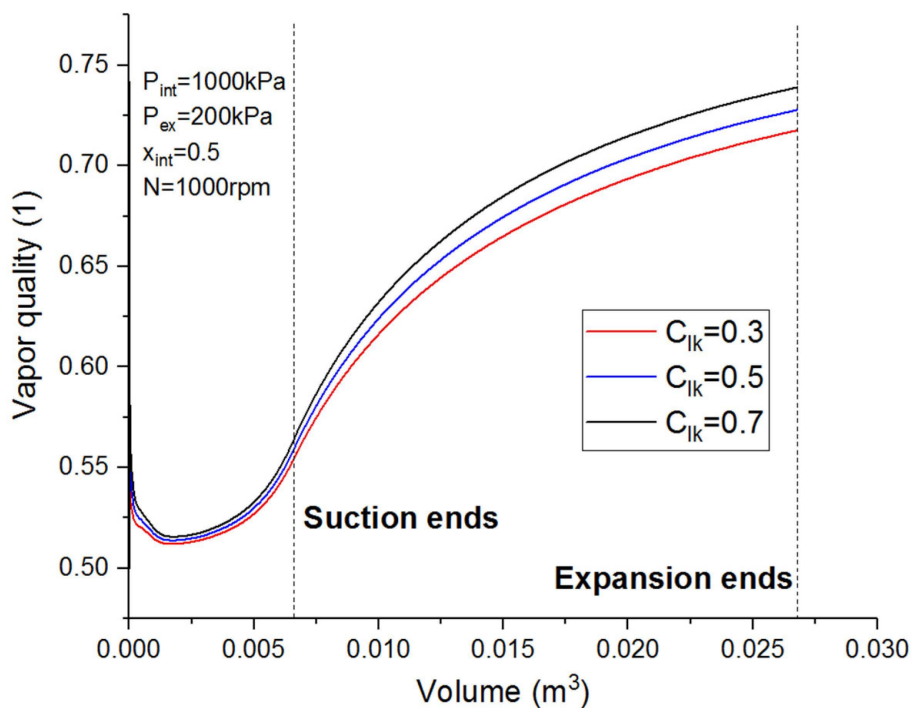
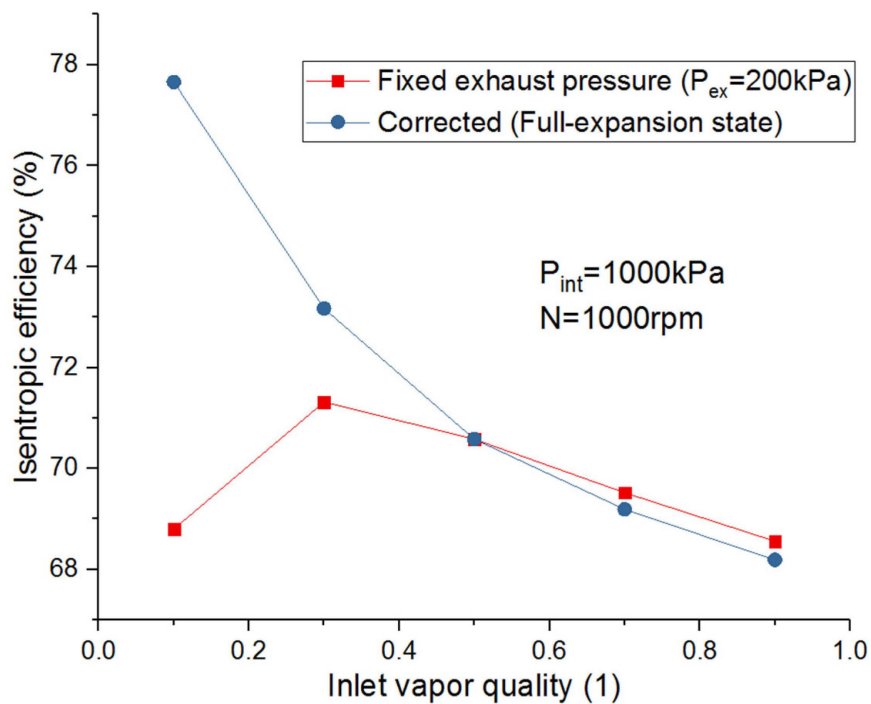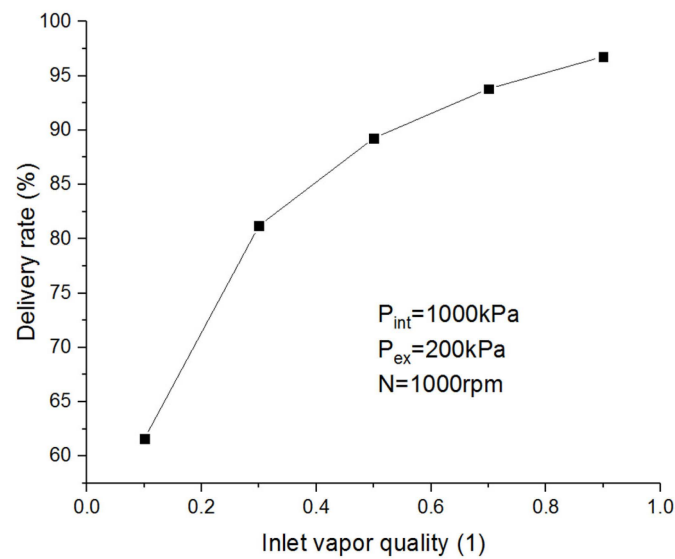**Figure 16.** The influence of leakage on the vapor quality variation (water).

Figure 17. The influence of inlet vapor quality on isentropic efficiency (water).

Figure 18. The influence of inlet vapor quality on delivery rate (water).

The output power decreased with increase in inlet vapor quality, as illustrated by the P-V diagram. It can be seen from Figure 10 that, with the increase in inlet vapor quality, the P-V area became smaller, which led to smaller output power. This can also be explained in a thermodynamic way. As explained in Figures 11–13, the vapor mass changed very little when inlet vapor quality changed. Therefore, the work done by the vapor was almost constant. However, for smaller inlet vapor quality, more liquid mass entered the expander and more vapor flash evaporated from the liquid. Therefore, more work was done by the flash vapor. That is why the output work was higher for lower inlet vapor quality. However, one thing that should be noted is that, although the output power decreased with increase in inlet vapor quality, the output power per unit of mass increased, as shown in Figure 19. For a fixed volume flow rate, the intake mass flow rate decreased sharply with increase in vapor quality, while the major work produced by the vapor changed little. Therefore, it was concluded that if the volume flow rate was fixed, lower inlet vapor quality was better to maximize the output work. However, if the mass flow rate was fixed, higher inlet vapor quality was better.
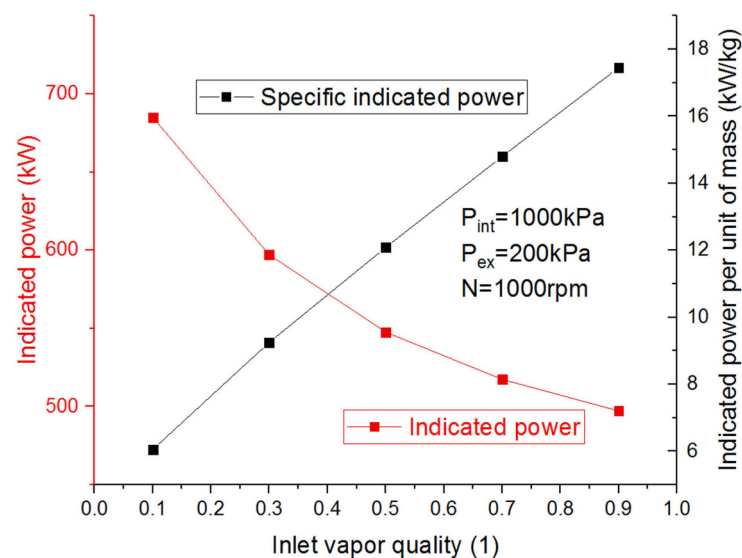
Figure 19. The influence of inlet vapor quality on output work rate per unit of mass (water).

In conclusion, for a two-phase fluid expander, more fluid flow admission and less leakage loss can be expected. More importantly, much higher volumetric expansion ratios of the working fluid are achievable as a result of the high density of two-phase fluids and the expansion starting upstream of the working chamber. Thus, overall fluid volumetric expansion ratios of up to the order of 25–30:1 in the machine can be achieved with pure liquid admission, which makes the two-phase volumetric expander more favorable.

3.3. The Influence of Rotating Speed

The influence of rotating speed on the expander is investigated using the developed model in this section. The working conditions were set as $P_{int} = 1\text{MPa}, P_{ex} = 0.2 \text{ MPa},$ $x_{int} = 0.5$.

Figure 20 shows the influence of the rotating speed on the working process of the expander. It can be clearly seen that the pressure during the intake phase decreased as the rotating speed increased. The reason was that, when the rotating speed increased, the momentum of the admitted fluid increased, which led to the greater pressure drop during the intake phase. As a result, the vapor pressure during the intake phase reduced and, accordingly, the density of the fluid reduced, thus decreasing the intake mass in the working volume, as shown in Figure 21.

Figure 21 shows the mass variation in the working volume. It can be seen that both the intake mass and leakage mass decreased as the rotating speed increased. The leakage mass decreased just because of the reduced flow time.

In conclusion, the intake mass and leakage mass both decreased as the rotating speed increased. Therefore, according to the definition, the delivery rate would decrease because of the reduced intake mass and leakage mass, as shown in Figure 22. It should be noted that the delivery rate could be larger than 1 because of leakage during the intake phase.

As can be seen from Figure 22, the indicated isentropic efficiency $\eta_{i,s}$ increased as the rotation speed increased, which largely resulted from the reduced leakage mass. However, the increasing rotation speed also increased the pressure drop at the same time. Considering that the increasing rotation speed would also increase mechanical losses and hydraulic losses, including frictional loss and acceleration loss, there should be an optimal rotation speed to maximize the effective isentropic efficiency $\eta_{e,s}$.
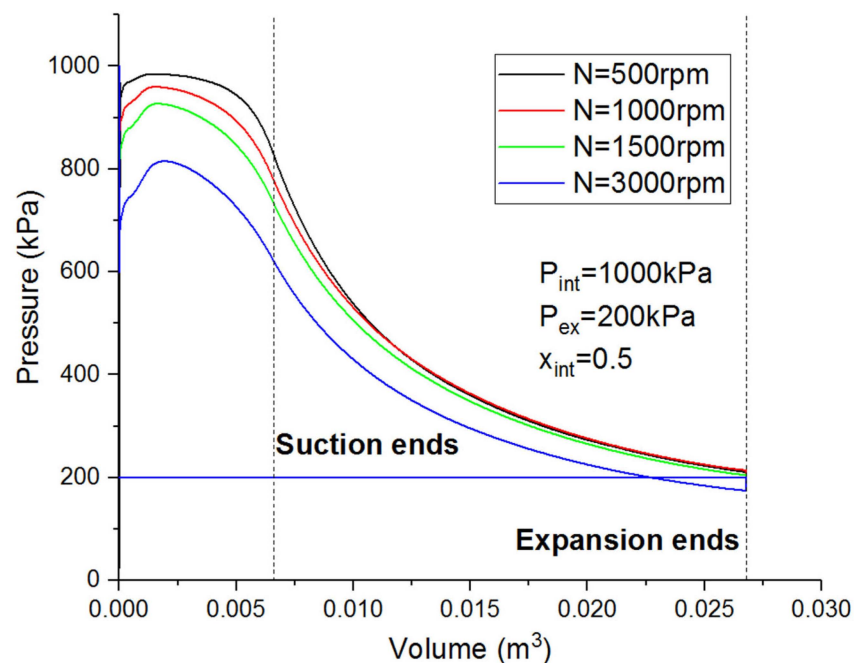

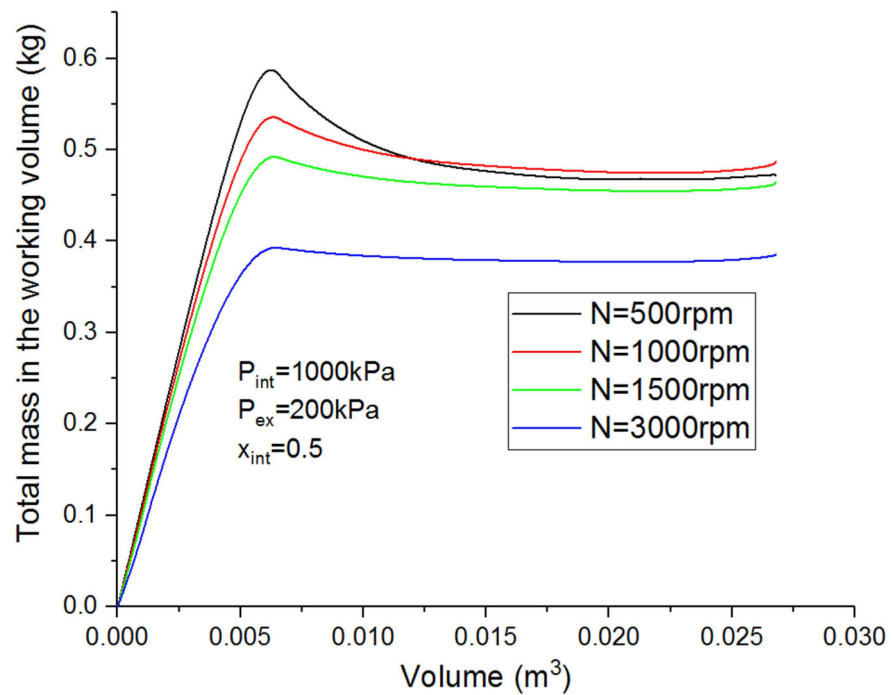**Figure 20.** The influence of rotating speed on the working process (water).

Figure 21. The influence of rotating speed on the mass in the working volume (water).
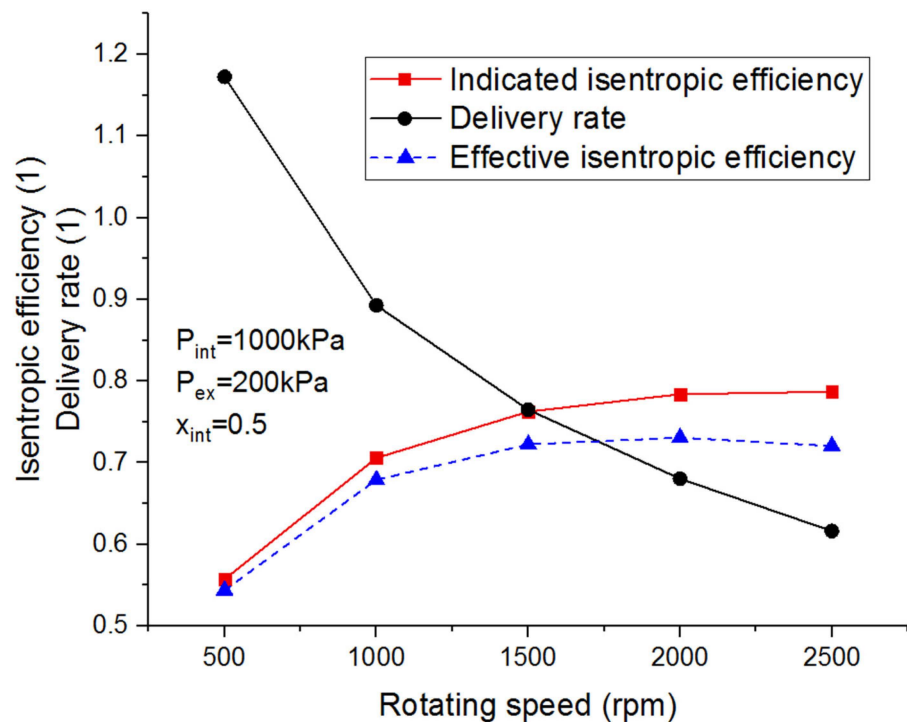

Figure 22. The influence of rotating speed on volumetric efficiency (water).

The influence of rotating speed on the expander output power is shown in Figure 23. The increasing rotation speed caused a larger mass flow rate, which always led to an increase in the output work (at least in a wide range of rotation speeds). However, the precondition was that the incoming mass flow rate was high enough. As for the indicated power per unit of mass, it remained nearly unchanged when the rotation speed was high enough.
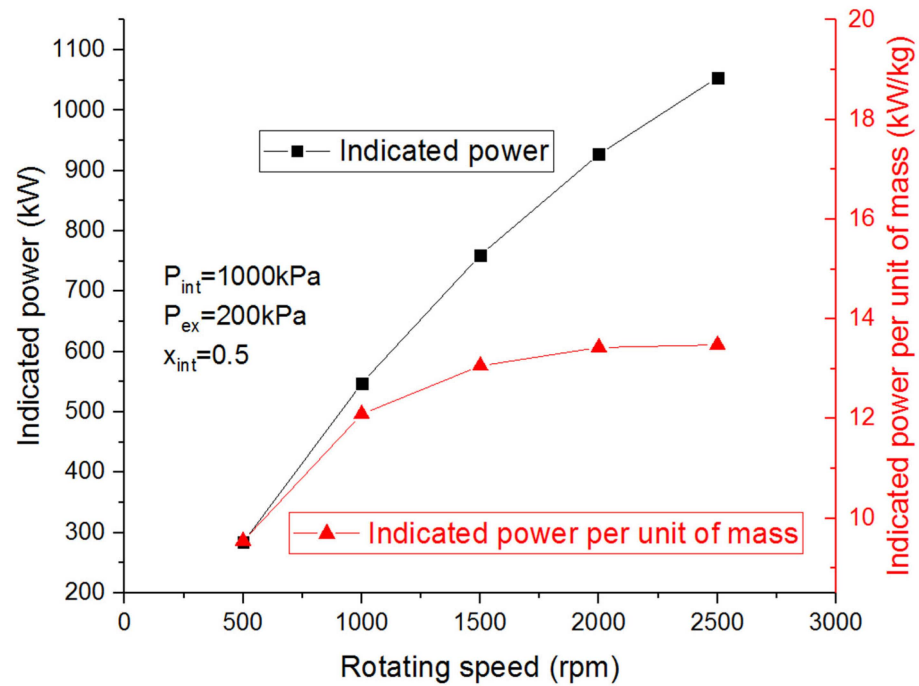
Figure 23. The influence of rotating speed on expander output power.

3.4. The Influence of Intake and Exhaust Pressure

To investigate the influence of intake pressure, the working conditions were set as $x_{int} = 0.5$, $P_{ex} = 0.2$ MPa, N = 1000 rpm.

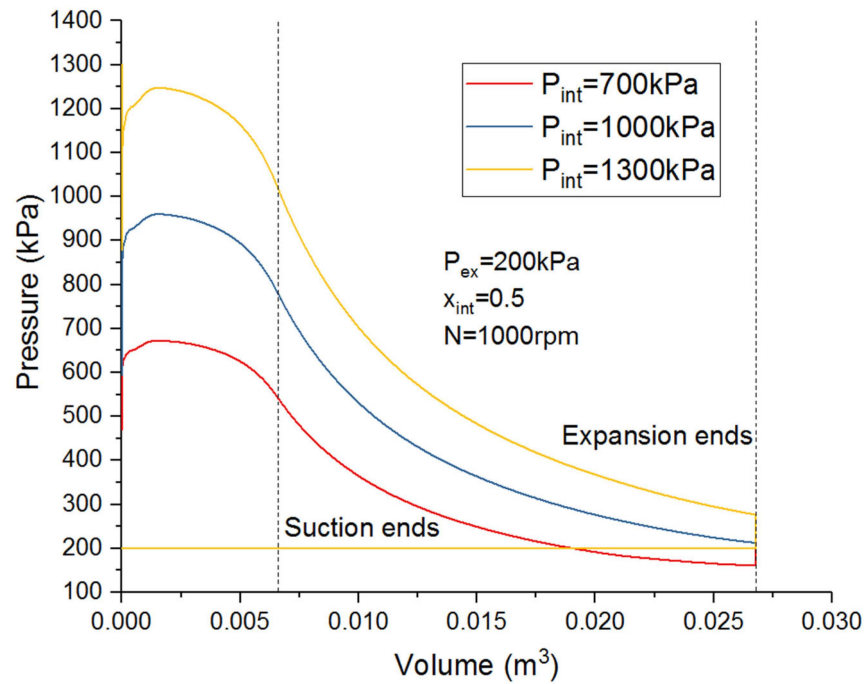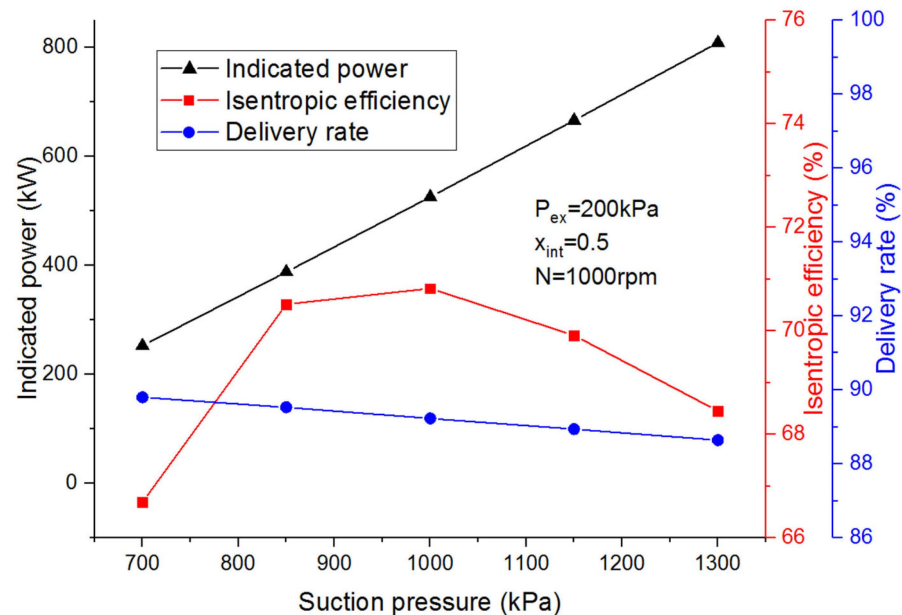The influence of intake pressure on the working process of the expander is shown in Figure 24.

Figure 24. The influence of intake pressure on working process.

It can be seen from Figure 25 that, for $P_{int} = 1000$ kPa, the working process was at full-expansion state, which means the pressure in the working chamber at the end of expansion phase was equal to the exhaust pressure. For $P_{int} = 1300$ kPa and $P_{int} = 700$ kPa, under-

expansion and over-expansion occurred, respectively, which would reduce the isentropic efficiency. However, for the output work, it was apparent that the higher intake pressure led to a larger P-V area and, therefore, larger output work. The higher intake pressure led to larger intake density, which would slightly reduce the delivery rate. The performance of the expander depended on different intake pressures, as shown in Figure 25.

Figure 25. The influence of intake pressure on expander performance.

It can also be seen from Figure 25 that under-expansion had relatively little influence on isentropic efficiency and presented better performance than over-expansion, in terms of isentropic efficiency. Therefore, a slightly higher intake pressure is acceptable in practice. This conclusion is consistent with Ref. [15].

The influence analysis of exhaust pressure on expander performance was similar with that of intake pressure. The lower exhaust pressure always led to higher output power; However, the exhaust pressure meeting full-expansion requirements presented the largest isentropic efficiency; The exhaust pressure also had no significant impact on delivery rate.

However, in practice, the ideal value for the exit pressure value is a bit higher than that in the discharge pipe, leading to some under-expansion in the machine itself. By this means, the built-in volume ratio of the working chamber can be reduced, thereby allowing a greater mass flow through the machine and, hence, increased power output and reduced machine size and cost. The loss in power output and efficiency due to this under-expansion is more than compensated for by the reduction in relative leakage rates, leading, overall, to increased power output and a more efficient and cheaper machine.

4. Conclusions

A specific twin-screw expander is explored under two-phase expansion conditions in this paper. The working process of two-phase expansion, including the leakage situation, is presented in detail. The factors of influence, including inlet vapor quality, rotating speed and intake pressure, are investigated using a developed model. Some useful conclusions for volumetric expanders can be drawn through the simulation.

1. The inlet vapor quality shows significant impact on the expander working process. The supply pressure drop is more serious for lower inlet vapor quality, due to the larger density in the liquid phase than in the vapor phase. Lower inlet vapor quality led to higher exhaust pressure at the end of the expansion phase, which may result in under-expansion.

2. The expander performance is also related to inlet vapor quality. The simulation showed that, under the full-expansion state, the isentropic efficiency was higher for lower vapor quality. This is because lower vapor quality leads to less leakage of the vapor phase. The simulation also showed that higher vapor quality led to a higher delivery rate. This is because the vapor phase can fill the working volume better than the liquid phase. As for the power output, the results showed that lower inlet vapor quality led to higher power output with a fixed volume flow rate. Nevertheless, for a fixed mass flow rate, higher power output is achieved with higher inlet vapor quality.

3. It was also found that the leakage situation influences the vapor quality variation in the expander. A more serious leakage situation leads to higher vapor quality at the discharge port.

In conclusion, more fluid flow admission, less leakage loss and much higher volumetric expansion ratios of the working fluid are achievable, which increases the usefulness of the two-phase volumetric expander.

Author Contributions: Modeling, data analysis, writing, editing, Y.M.; programming, editing, review, Y.Z.; numerical computation, Z.Z. All authors have read and agreed to the published version of the manuscript.

Data Availability Statement: The data presented in this study are available on request from the corresponding author.

Conflicts of Interest: The authors declare no conflict of interest.

Nomenclature

Latin symbols		**Greek letters**	
A	flow area, m^2	η	efficiency, 1
C	flow coefficient, 1	ρ	density, kg/m^3
G	mass, kg	**Subscripts**	
h	specific enthalpy, J/kg	e,eff	effective
$\dot{m}$	mass flow rate, kg/s	ex	exhaust phase
N	rotating speed, rpm	g	gas
p	pressure, kPa or MPa	ie	end of intake phase
P	power, kW	in	flow in
Q	mass flow rate, kg/s	i, ind	indicated
s	specific entropy, J/(kg·K)	int	intake phase
T	temperature, K	is	start of intake phase
t	time, s	l	liquid
u	specific internal energy, kJ/kg	lk	leakage
V	volume, m^3	m	mechanical loss
w	work, kJ	mr	male rotor
x	vapor quality, 1	out	flow out
z	number of lobes, 1	s	isentropic
		tp	two-phase

References

1. Chicco, J.M.; Fonte, L.; Mandrone, G.; Tartaglino, A.; Vacha, D. Hybrid (Gas and Geothermal) greenhouse simulations aimed at optimizing investment and operative costs: A case study in NW Italy. *Energies* **2023**, *16*, 3931. [CrossRef]
2. El-Sebaey, M.S.; Ellman, A.; El-Din, S.S.; Essa, F.A. Thermal performance evaluation for two designs of flat-plate solar air heater: An experimental and CFD investigations. *Processes* **2023**, *11*, 1227. [CrossRef]
3. Wang, W.; Wu, Y.T.; Ma, C.F.; Liu, L.D.; Yu, J. Preliminary experimental study of single screw expander prototype. *Appl. Therm. Eng.* **2011**, *31*, 3684–3688. [CrossRef]

4. Murthy, A.A.; Norris, S.; Subiantoro, A. Performance of a four-intersecting-vane expander in a R134a refrigeration cycle. *Appl. Therm. Eng.* **2022**, *209*, 118244. [CrossRef]

5. Imran, M.; Usman, M.; Park, B.S.; Lee, D.H. Volumetric expanders for low grade heat and waste heat recovery applications. *Renew. Sustain. Energy Rev.* **2016**, *57*, 1090–1109. [CrossRef]

6. Li, T.; Zhu, J.; Fu, W.; Hu, K. Experimental comparison of R245fa and R245fa/R601a for organic Rankine cycle using scroll expander. *Int. J. Energy Res.* **2015**, *39*, 202–214. [CrossRef]

7. Ali Tarique, M.; Dincer, I.; Zamfirescu, C. Experimental investigation of a scroll expander for an organic Rankine cycle. *Int. J. Energy Res.* **2014**, *38*, 1825–1834. [CrossRef]

8. Li, G.; Lei, B.; Wu, Y.; Zhi, R.; Zhao, Y.; Guo, Z.; Liu, G.; Ma, C. Influence of inlet pressure and rotational speed on the performance of high pressure single screw expander prototype. *Energy* **2018**, *147*, 279–285. [CrossRef]

9. Zhang, Y.Q.; Wu, Y.T.; Xia, G.D.; Ma, C.F.; Ji, W.N.; Liu, S.W.; Yang, K.; Yang, F.B. Development and experimental study on organic Rankine cycle system with single-screw expander for waste heat recovery from exhaust of diesel engine. *Energy* **2014**, *77*, 499–508. [CrossRef]

10. Lemort, V.; Quoilin, S.; Cuevas, C.; Lebrun, J. Testing and modeling a scroll expander integrated into an Organic Rankine Cycle. *Appl. Therm. Eng.* **2009**, *29*, 3094–3102. [CrossRef]

11. Quoilin, S.; Lemort, V.; Lebrun, J. Experimental study and modeling of an Organic Rankine Cycle using scroll expander. *Appl. Energy* **2010**, *87*, 1260–1268. [CrossRef]

12. Giuffrida, A. Improving the semi-empirical modelling of a single-screw expander for small organic Rankine cycles. *Appl. Energy* **2017**, *193*, 356–368. [CrossRef]

13. Wu, Z.; Pan, D.; Gao, N.; Zhu, T.; Xie, F. Experimental testing and numerical simulation of scroll expander in a small scale organic Rankine cycle system. *Appl. Therm. Eng.* **2015**, *87*, 529–537. [CrossRef]

14. Smith, I.K.; Stosic, N.; Kovacevic, A. Modelling and performance calculation of screw expanders. In *Power Recovery from Low Grade Heat by Means of Screw Expanders*; Elsevier: Amsterdam, The Netherlands, 2014; pp. 93–125.

15. Tang, H.; Wu, H.; Wang, X.; Xing, Z. Performance study of a twin-screw expander used in a geothermal organic Rankine cycle power generator. *Energy* **2015**, *90*, 631–642. [CrossRef]

16. Papes, I.; Degroote, J.; Vierendeels, J. New insights in twin screw expander performance for small scale ORC systems from 3D CFD analysis. *Appl. Therm. Eng.* **2015**, *91*, 535–546. [CrossRef]

17. Papes, I.; Degroote, J.; Vierendeels, J. Development of a thermodynamic low order model for a twin screw expander with emphasis on pulsations in the inlet pipe. *Appl. Therm. Eng.* **2016**, *103*, 909–919. [CrossRef]

18. He, W.; Wu, Y.; Peng, Y.; Zhang, Y.; Ma, C.; Ma, G. Influence of intake pressure on the performance of single screw expander working with compressed air. *Appl. Therm. Eng.* **2013**, *51*, 662–669. [CrossRef]

19. Lei, B.; Wang, W.; Wu, Y.T.; Ma, C.F.; Wang, J.F.; Zhang, L.; Li, C.; Zhao, Y.K.; Zhi, R.P. Development and experimental study on a single screw expander integrated into an Organic Rankine Cycle. *Energy* **2016**, *116*, 43–52. [CrossRef]

20. Marami Milani, S.; Khoshbakhti Saray, R.; Najafi, M. Exergo-economic analysis of different power-cycle configurations driven by heat recovery of a gas engine. *Energy Convers. Manag.* **2019**, *186*, 103–119. [CrossRef]

21. Lhermet, G.; Tauveron, N.; Caney, N.; Blondel, Q.; Morin, F. A recent advance on partial evaporating organic Rankine cycle: Experimental results on an axial turbine. *Energies* **2022**, *15*, 7559. [CrossRef]

22. Li, D.; He, Z.; Wang, Q.; Wang, X.; Wu, W.; Xing, Z. Thermodynamic analysis and optimization of a partial evaporating dual-pressure organic rankine cycle system for low-grade heat recovery. *Appl. Therm. Eng.* **2021**, *185*, 116363. [CrossRef]

23. Dawo, F.; Buhr, J.; Schifflechner, C.; Wieland, C.; Spliethoff, H. Experimental assessment of an Organic Rankine Cycle with a partially evaporated working fluid. *Appl. Therm. Eng.* **2023**, *221*, 119858. [CrossRef]

24. Taniguchi, H.; Kudo, K.; Park, I.; Kumazawa, S. Analytical and experimental investigation of two-phase flow screw expanders for power generation. *J. Eng. Gas Turbines Power* **1985**, *110*, 4. [CrossRef]

25. Wu, W.F.; Wang, Q.; Zhang, Z.; Wu, Z.J.; Yang, X.T.; Xu, L.C. Influence of evaporating rate on two-phase expansion in the piston expander with cyclone separator. *Therm. Sci.* **2020**, *24*, 2077–2088. [CrossRef]

26. Smith, I.K. Total flow and other systems involving two-phase expansion. In *Geothermal Power Generation*; Woodhead Publishing: Cambridge, UK, 2016; pp. 321–351.

27. Smith, I.K. Development of the trilateral flash cycle system. *Proc. Inst. Mech. Eng.* **1993**, *207*, 179–194. [CrossRef]

28. Smith, I.; Sto, N.; Aldis, C.A. Development of the trilateral flash cycle system. Part 3: The design of high-efficiency two-phase screw expanders. *Proc. Inst. Mech. Eng. Part A J. Power Energy* **1996**, *210*, 75–93. [CrossRef]

29. Xia, G.D.; Zhang, Y.Q.; Wu, Y.T.; Ma, C.F.; Ji, W.N.; Liu, S.W.; Guo, H. Experimental study on the performance of single-screw expander with different inlet vapor dryness. *Appl. Therm. Eng.* **2015**, *87*, 34–40. [CrossRef]

30. Nikolov, A.; Brümmer, A. Two-phase mass flow rate through restrictions in liquid-flooded twin-screw compressors or expanders. *Int. J. Refrig.* **2023**, *148*, 152–167. [CrossRef]

31. Bianchi, G.; Kennedy, S.; Zaher, O.; Tassou, S.A.; Miller, J.; Jouhara, H. Numerical modeling of a two-phase twin-screw expander for Trilateral Flash Cycle applications. *Int. J. Refrig.* **2018**, *88*, 248–259. [CrossRef]

32. Bianchi, G.; Marchionni, M.; Miller, J.; Tassou, S.A. Modelling and off-design performance optimisation of a trilateral flash cycle system using two-phase twin-screw expanders with variable built-in volume ratio. *Appl. Therm. Eng.* **2020**, *179*, 115671. [CrossRef]

33. Smith, S.L. Void fractions in two-phase flow: A correlation based upon an equal velocity head model. *Thermodyn. Fluid Mech. Group* **1969**, *184*, 647–664. [CrossRef]
34. Lemmon, E.W.; Huber, M.L.; McLinden, M.O. *NIST Reference Fluid Thermodynamic and Transport Properties—REFPROP User's Guide*; NIST: Gaithersburg, MD, USA, 2013.
35. Nikolov, A.; Brümmer, A. Investigating a small oil-flooded twin-screw expander for waste-heat utilisation in organic Rankine cycle systems. *Energies* **2017**, *10*, 869. [CrossRef]